J Mater Sci (2010) 45:6417–6423
DOI 10.1007/s10853-010-4725-8

Synthesis and photoluminescence of Eu-doped Zn/Al layered double hydroxides

Yufeng Chen · Songhua Zhou · Fan Li · Yiwang Chen

Received: 17 March 2010 / Accepted: 16 June 2010 / Published online: 29 June 2010

Abstract Eu-doped ZnAl-layered double hydroxides (ZnAl–LDHs) with various $Zn^{2+}/(Al^{3+}+Eu^{3+})$ molar ratios from 1:1, 2:1, 3:1, to 4:1 were first synthesized by the coprecipitation method at room temperature and the Eu^{3+}/Al^{3+} molar ratio of 0.06 was almost maintained. The obtained solids were characterized by powder X-ray diffraction (XRD), photoluminescent spectrum (PL), scanning electron microscope (SEM), infrared spectroscopy (IR), and thermogravimetric (TG) analysis. XRD results show that the crystallinity of the Eu-doped products gradually was improved when the $Zn^{2+}/(Al^{3+}+Eu^{3+})$ molar ratio was higher than 2. The photoluminescent spectra of the Eu-doped ZnAl–LDHs are described by the well-known $^5D_0$–^7F_J transition ($J = 1, 2, 3, 4$) of Eu^{3+} ions with the strongest emission for $J = 2$.

Introduction

Studies on layered double hydroxides (LDHs), known as hydrotalcite-like anionic clays materials, have been conducted over the past several decades since they have many possibilities of the applications for anion exchangers, catalysts, biosensor, and the immobilization hosts of functional molecules by intercalation into their layers [1–5]. LDHs consist of positively charged brucite-like layers, where a fraction of the divalent cations was replaced by trivalent cations. The positively charged layers were separated by the charge-balancing anions and water molecules [6]. Up to the present time, most of studies on LDHs were focused on ion-exchange [7], organic-intercalation [8, 9], and exfoliation/self-assembly [10], etc. For the application of fluorescent probe in biology or medical diagnosis, rare earth ions doped into LDHs should be meaningful. In fact, with rare earth-based host layers and tunable interlayer guests, the rare earth-doped LDHs compounds may be of interest not only for biomedical materials but also for magnetic, catalytic, and optoelectronic materials, etc.

Rare earth complexes, especially those containing europium and terbium, have been the subject of extensive research because of their sharp and intense emission bands arising from *f–f* transitions [11, 12]. Recently, some attempts to intercalate rare earth ions complex into interlayer of LDH have been reported [13–17], and some layered rare earth hydroxides have been investigated [18–21]. Lee et al. have successfully synthesized the rare earth hydroxides of $RE(OH)_{2.5}(NO_3)_{0.5} \cdot xH_2O$ (RE = Gd, Eu, and Sm) by a hydrothermal reaction and studied ion-exchange reactivity between NO_3^- and diverse organic anions [18]; Monge and coworkers [19] have also successfully prepared two ytterbium catalytically active MOF materials which are bifunctional catalysts in redox and acid processes; Geng et al. [20, 21] have reported the synthesis of a series of rare earth layered hydroxides with a composition of $RE(OH)_{2.5}Cl_{0.5}0.8H_2O$ (RE: Eu, Tb, etc.) through the homogeneous precipitation of $RECl_3xH_2O$ with hexa-methylenetetramine (HMT).

As we all know, the rare earth elements are expensive compared with that of the common elements. With the views of the cheap materials and application, it is

Y. Chen (✉) · S. Zhou · Y. Chen (✉)
Department of Chemistry, Nanchang University, Nanchang 330031, China
e-mail: yfchen@ncu.edu.cn

Y. Chen
e-mail: ywchen@ncu.edu.cn

F. Li · Y. Chen
Institute of Polymers Nanchang University, Nanchang 330031, China

worthwhile to investigate the RE-doped LDHs. However, to the best of our knowledge, the study on the RE ions doped into layers of LDH was hardly reported. In this paper, we first reported the Eu ions doped into layers of Zn/Al–LDH. It is very important as a fluorescent probe for the potential application in biology or medical diagnosis by various photoluminescent properties resulted from different interlayer guests. This probe fabricated with inorganic materials should have more high thermal stability and less toxicity compared with those probes fabricated with organic materials.

Experimental procedure

$ZnCl_2$, $AlCl_3 \cdot 6H_2O$, Eu_2O_3, $NH_3 \cdot H_2O$, and HCl were of A.R. grade, and were purchased from Chemistry Reagent Corporation of National Medicine Group. CO_2-free deionized water was used in all experiments. $ZnCl_2$ and $AlCl_3 \cdot 6H_2O$ were dissolved in CO_2-free deionized water to make into 0.5 mol $\cdot L^{-1}$ $ZnCl_2$ and 0.25 mol $\cdot L^{-1}$ $AlCl_3$ solution, respectively. And $EuCl_3$ (0.06 mol $\cdot L^{-1}$) solution was prepared with 12 mol $\cdot L^{-1}$ HCl and CO_2-free deionized water. Then Eu-doped ZnAl–Cl LDHs with starting $Zn^{2+}/(Al^{3+}+Eu^{3+})$ molar ratios of 1/1, 2/1, 3/1, and 4/1, and an $Eu^{3+}/(Al^{3+}+Eu^{3+})$ ratio of 0.06 were prepared by the coprecipitation method [22]. The procedure was as follows: $NH_3 \cdot H_2O$ solution was gradually added to the mixed solutions (pH = 1–2) of $ZnCl_2$, $AlCl_3$, and $EuCl_3$ with certain molar ratios and continuous stirring. After precipitation (pH $\approx$ 8), the slurry was filtrated, washed with CO_2-free deionize water, and dried at 70 °C for 12 h. The Eu-doped ZnAl–Cl–LDHs prepared from starting $Zn^{2+}/(Al^{3+}+Eu^{3+})$ molar ratios of 1/1, 2/1, 3/1, and 4/1 were signed as Zn_1–AlEu, Zn_2–AlEu, Zn_3–AlEu, and Zn_4–AlEu, respectively. The undoped ZnAl–Cl–LDH with starting Zn^{2+}/Al^{3+} molar ratio of 2/1 was prepared by the same method as above and signed as Zn_2–Al.

All measurements for characterization were performed at room temperature. X-Ray powder diffraction (XRD) patterns were recorded on a Bruker D8 Focus (40 kV, 40 mA) with Cu-K_α radiation. The XRD patterns of all the samples were measured with step size of 0.02°, scanning rate of 2°/min, and 2θ ranging from 4.0° to 70°. The Fourier Infrared spectra (FTIR) of the samples were obtained with Shimadzu IR Prestige-21 FTIR spectrometer by the KBr method.

Chemical contents of Zn, Al, and Eu were determined by inductively coupled plasma atomic emission spectroscopy (ICP-AES, OPTIMA 5300DV, AMERICAN PE COMPANY). Thermogravimetry (TG), differential thermogravimetry (DTG), and differential thermal analysis (DTA) data were collected using synchronous thermal analyzer (PYRIS DIAMOVD, AMERICAN PE COMPANY). The chemistry formula was estimated from the results of ICP and TG analyses.

Scanning electron microscope (SEM) observation was carried out using a Quanta 200 FEG (FEI COMPANY) operated at 20.00 kV. The photoluminescent property of the samples was studied with the help of F-4600 FL Spectrophotometer.

Results and discussion

The $Zn^{2+}/(Al^{3+}+Eu^{3+})$ ratios in the precipitates were given in Table 1. There was a slight discrepancy between calculated and observed ratios, indicating that almost all Zn, Al, and Eu ions were almost precipitated during synthesis. The estimated formula considers that chloride is the only compensating anion and does not take into account the presence of small carbonate impurities in the interlayer

Table 1 Determination of Zn/(A1+Eu) ratios by chemical analyses and of a and c parameters for the original precipitate

Samples	$Zn^{2+}/(Al^{3+}+Eu^{3+})$ ratio		Eu^{3+}/Al^{3+} ratio	Cell parameters and Hexagonal symmetry		
	$^{+}$Cal.	$^{++}$Obs.	$^{+}$Cal.($^{++}$Obs.)	a (Å)	c (Å)	d_{003} spacing
Zn_2–Al	2.0	1.97	0(0)	3.095 (2)	23.49 (2)	7.85
	Formula	$Zn_2Al(OH)_6Cl \cdot 1.2H_2O$				
Zn_1–AlEu	1.0	0.98	0.06 (0.061)			7.82
Zn_2–AlEu	2.0	1.93	0.06 (0.059)	3.097 (2)	23.50 (3)	7.85
	Formula	$Zn_2Al_{0.94}Eu_{0.06}(OH)_6Cl \cdot 1.2H_2O$				
Zn_3–AlEu	3.0	2.98	0.06 (0.063)	3.098 (2)	23.52 (1)	7.86
Zn_4–AlEu	4.0	3.96	0.06 (0.064)	3.101 (4)	23.55 (6)	7.90

$^{+}$ Calculated for charged materials, $^{++}$ Observed for the precipitation

space (seen in Table 1). The crystallographic parameters, *a* and *c*, of the ternary Zn–Al–Eu LDHs and binary Zn–Al LDH were calculated using the least squares method assuming a hexagonal crystal system, where the *c* parameter corresponds to 3 times the distance between adjacent brucite-like layers, and the *a* parameter is almost the same as that of brucite (3.10 Å) (shown in Fig. 1). The interlayer distance, *d*, is approximately 7.9 Å. This value is in the literature range [23–25]. The *a* parameter increased as the Zn/A1 ratio increased due to substitution of the Al cation ($r = 0.53$ Å) by the larger Zn cation ($r = 0.745$ Å).The *c* parameter also increased with the increasing substitution. Since the synthetic parameters were kept constant for all the compounds, while varying only the composition of the metal ions, the increase in the *c* parameter is due to an increase of Zn content. Based on the electrostatic interactions between the layers and the anions, the larger interlayer distance was found for the sample with the higher $Zn^{2+}/(Al^{3+}+Eu^{3+})$ ratio which posses of lower charge density. So the *c* parameter of LDHs gradually increases with the increasing ratio of the $Zn^{2+}/(Al^{3+}+Eu^{3+})$. In addition, both *a* and *c* parameters slightly increased after the substitution of the Zn cation ($r = 0.745$Å) by the bigger Eu cation ($r = 0.95$ Å).

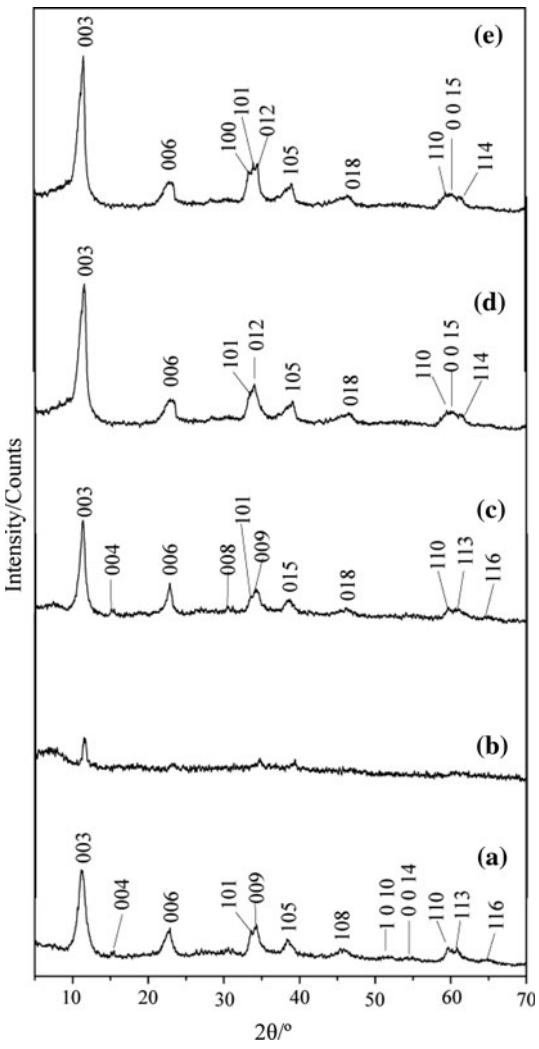

Fig. 1 XRD of (*a*) Zn_2–Al, (*b*) Zn_1–AlEu, (*c*) Zn_2–AlEu, (*d*) Zn_3–AlEu, and (*e*) Zn_4–AlEu, respectively

The crystallinity of the Eu-doped products depends on the $Zn^{2+}/(Al^{3+}+Eu^{3+})$ molar ratios. No diffraction lines were observed as the $Zn^{2+}/(Al^{3+}+Eu^{3+})$ molar ratio was of 1/2 (Figure not shown here). With the $Zn^{2+}/(Al^{3+}+Eu^{3+})$ molar ratio increased from 1/1, 2/1, 3/1, to 4/1, the diffraction peak intensity became stronger. Namely, the crystallinity of the product was improved when the $Zn^{2+}/(Al^{3+}+Eu^{3+})$ ratio was in excess of the 2/1, which is very similar to that of the undoped ZnAl–Cl LDH [25]. Patzko′ et al. [26] have studied the synthesis of ZnAl–LDHs with various Zn/Al ratios from 1:1 to 4:1 by the sol–gel method, and observed some peaks at 30°–40° attributed to ZnO phase as Zn/Al ratios increasing to 2:1 and 4:1 for their samples. However, this case did not occur for our products, which may be due to the different starting materials and synthetic processing. No diffraction peaks attributed to europium salts was observed, suggesting the Eu^{3+} ions incorporated in the framework of LDHs. All the XRD patterns of the undoped ZnAl–LDH and Eu-doped ZnAl–LDHs were similar to that of the literature ZnAl–Cl–LDHs [24, 25, 27].

The TG–DTA–DTG curves of representative samples were shown in Fig. 2. The results of the thermogravimetric analyses were summarized in Table 2. The mass losses of LDHs started at room temperature and completed at around 650 °C. Figure 2 showed similar thermal characters of the Zn_2–Al and Zn_2–AlEu, indicating the similar structure. Theoretically, three major mass losses should be observed. However, three mass losses were observed clearly in the TG–DTG curves of the representative samples. The first loss step happened at 70 and 85 °C with mass losses of 6.8 and 6.7% for the Zn_2–Al and Zn_2–AlEu, respectively, corresponding to the loss of the adsorbed water and the interlayer water. The second loss step took place at around 230 and 250 °C with mass losses of 14.2 and 13.9% for the Zn_2–Al and Zn_2–AlEu, respectively, attributed to the dehydroxylation of layers and small carbonate anions impurities. The third loss step with mass losses of 11.5 and 11.3% took place at 494 and 510 °C for the Zn_2–Al and Zn_2–AlEu, respectively, most probably due to the elimination of Cl^- intercalated in the LDH interlayers.

Based on the thermogravimetric analyses and phase transitions of ZnAl–LDHs depending on annealing temperatures (published elsewhere) between room temperature and 700 °C, the decomposition of the samples can be concluded as:

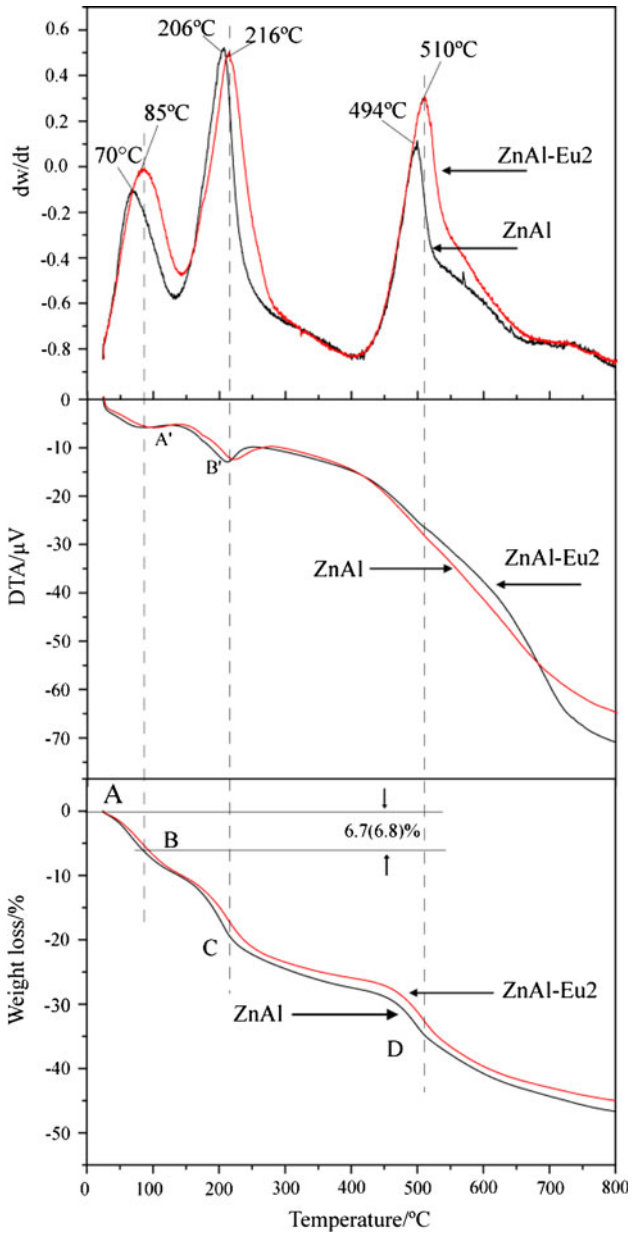

Fig. 2 TG–DTA–DTG curves of Zn_2–Al and Zn_2–AlEu

$$Zn_2Al(OH)_6Cl \cdot 1.2H_2O = Zn_2Al(OH)_6Cl + 1.2H_2O \quad (1)$$

$$Zn_2Al(OH)_6Cl = 2ZnO + 1/2Al_2O_3 + 5/2H_2O + HCl \quad (2)$$

$$Zn_2Al_{0.94}Eu_{0.06}(OH)_6Cl \cdot 1.2H_2O = Zn_2Al_{0.94}Eu_{0.06}(OH)_6Cl + 1.2H_2O \quad (3)$$

$$Zn_2Al_{0.94}Eu_{0.06}(OH)_6Cl = 2ZnO + 0.94/2\ Al_2O_3 + 0.06/2\ Eu_2O_3 + 5/2H_2O + HCl \quad (4)$$

Reaction (1) corresponds to the loss of the adsorbed water and the interlayer water of Zn_2–Al LDH, and reaction (2) corresponds to the dehydroxylation of layers and the elimination of Cl^- intercalated in the Zn_2–Al LDH. In the same way, reactions (3) and (4) correspond to the losses of the adsorbed and interlayer water, and the dehydroxylation of layers and the elimination of Cl^- intercalated in the Zn_2–AlEu LDH, respectively. These results indicated that the thermogravimetric analyses were in agreement with the chemical formulas. According to the results of thermogravimetric analyses, the obtained LDHs presented better thermal stability than those reported by other authors [28–30].

The FT-IR spectra of the LDHs samples were shown in Fig. 3. An intense and broad peak at 3490 cm^{-1} was ascribed to the stretching vibration of hydroxyl groups of LDH layers and interlayer water molecules [31]. The deformation vibration of water molecules was responsible for the band at 1619 cm^{-1}. It is noteworthy that despite the use of CO_2-free deionized water in all experiments, a weak band in the region 1500–1400 cm^{-1} attributed to carbonate anions [3, 32] was observed, suggesting small carbonate anions adsorbed during the synthesis. The band around 2350 cm^{-1} was attributed to CO_2 contaminated during measurement [33]. The contamination could not be avoided with longer scanning time. The band around 1265 cm^{-1} may be due to ammonia adsorbed [34]. The Al–OH deformation mode was recorded as a shoulder at ca. 945 cm^{-1} and the band close to 584 cm^{-1} was due to both Al–OH and Zn–OH translational modes [35]. These results were in agreement with that of the XRD.

Figure 4 showed the photoluminescent spectra of the products under excitation at 380 nm. In the 520–720 nm spectral range, no emission occurred for the undoped ZnAl LDH, while the Eu-doped ZnAl-LDHs revealed the red-emitting characteristic of Eu^{3+} ions from the transitions $^5D_0$–^7F_J ($J = 1$–4) centered around at 593, 616, 654, and

Table 2 Results of mass losses of the TG–DTG for the selected samples

	Step 1		Step 2		Step 3		Total mass loss (%)
	Mass loss (%)	Temp. (°C)	Mass loss (%)	Temp. (°C)	Mass loss (%)	Temp. (°C)	
Zn_2–Al	6.8	70	14.2	230	11.5	494	32.5
Zn_2–AlEu	6.7	85	13.9	250	11.3	510	31.9

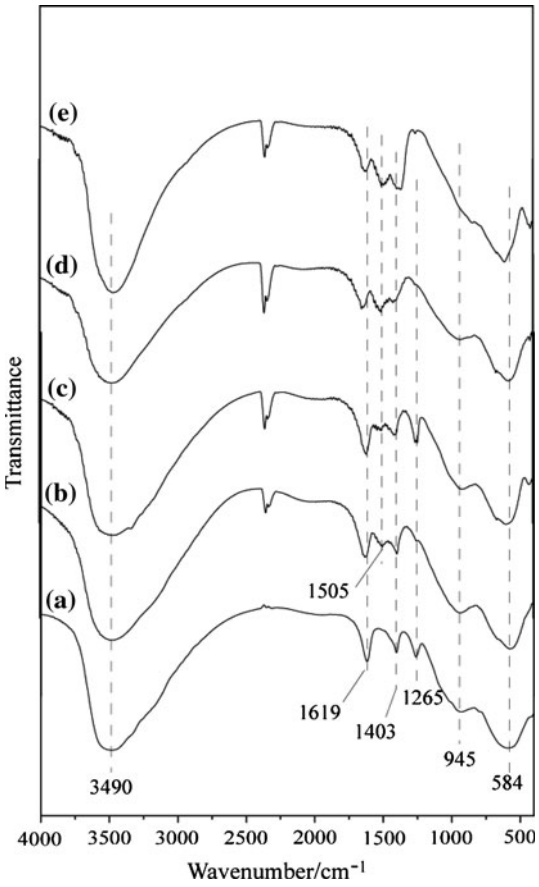

Fig. 3 IR spectra of (*a*) Zn_2–Al, (*b*) Zn_1–AlEu, (*c*) Zn_2–AlEu, (*d*) Zn_3–AlEu, and (*e*) Zn_4–AlEu, respectively

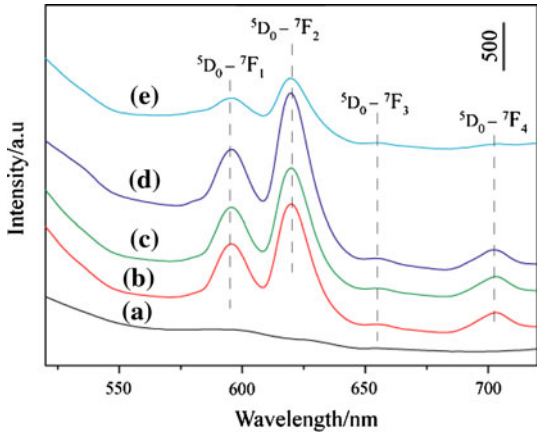

Fig. 4 Emission spectra of (*a*) Zn_2–Al, (*b*) Zn_1–AlEu, (*c*) Zn_2–AlEu, (*d*) Zn_3–AlEu, and (*e*) Zn_4–AlEu, respectively. ($\lambda_{ex} = 380$ nm)

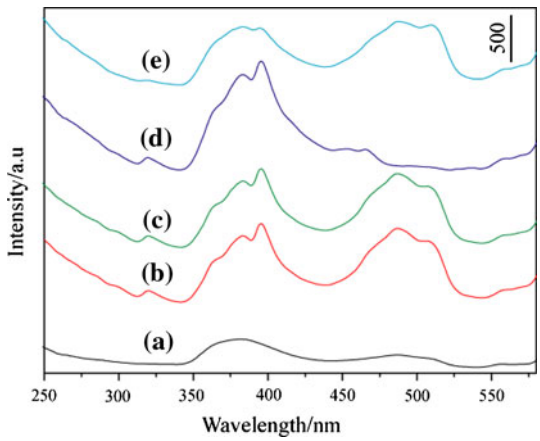

Fig. 5 Excitation spectra of (*a*) Zn_2–Al, (*b*) Zn_1–AlEu, (*c*) Zn_2–AlEu, (*d*) Zn_3–AlEu, and (*e*) Zn_4–AlEu, respectively. ($\lambda_{em} = 600$ nm)

700 nm, respectively. The narrow-band emission at 616 nm was characteristic of the hypersensitive $^5D_0$–$^7F_2$ transition of Eu^{3+}, which was much more intense than the $^5D_0$–$^7F_1$ transition at 593 nm. This observation was consistent with the fact that the Eu^{3+} centers did not possess inversion symmetry [36, 37]. As can be seen, the relative intensities spectral profiles of the $^5D_0$–^7F_J transitions ($J = 1$–4) were very similar, indicating that the Eu^{3+} ions were in similar chemical environments in the compounds. The transitions $^5D_0$–^7F_J ($J = 1$–4) were often observed in other Eu-doped systems and its photoluminescent spectrum (PL) intensity comes up to or even more than those of Eu-doped systems [16, 17, 38, 39]. Figure 5 showed the excitation spectra of the products with emission wavelength of 600 nm. The optimal excitation wavelength for all the samples was at 375–400 nm.

SEM micrographs of products were shown in Fig. 6. No obvious lamellar structure was observed in our samples. As the Zn/Al ratio increased to 4/1 from 1/1, the SEM images of the products almost did not change. Benito and Patzko′ have observed the lamellar structures of ZnAl–LDH with Zn/Al ratio of 2/1, but as the Zn/Al ratio increased to 3/1 and 4/1, some rod-like particles due to ZnO were detected [22, 26]. This difference in micrographs of products for different research groups may be due to different synthetic processes.

Conclusions

In conclusion, Eu-doped ZnAl-layer double hydroxides with various $Zn^{2+}/(Al^{3+}+Eu^{3+})$ ratios from 1:1 to 4:1 were prepared by the coprecipitation method. XRD, SEM, ICP, thermal analysis, infrared spectroscopy, and PL were powerful methods employed in the characterization of hydrotalcite-type materials. The effect of $Zn^{2+}/(Al^{3+}+Eu^{3+})$ ratios on the crystallinity of the hydrotalcite materials showed that adding the $Zn^{2+}/(Al^{3+}+Eu^{3+})$ ratios favored the formation of the hydrotalcite. The variation of $Zn^{2+}/(Al^{3+}+Eu^{3+})$ ratios showed that at low ratio no hydrotalcite-type structure formed, with the increase of $Zn^{2+}/(Al^{3+}+Eu^{3+})$ ratio, the crystallinity was improved.

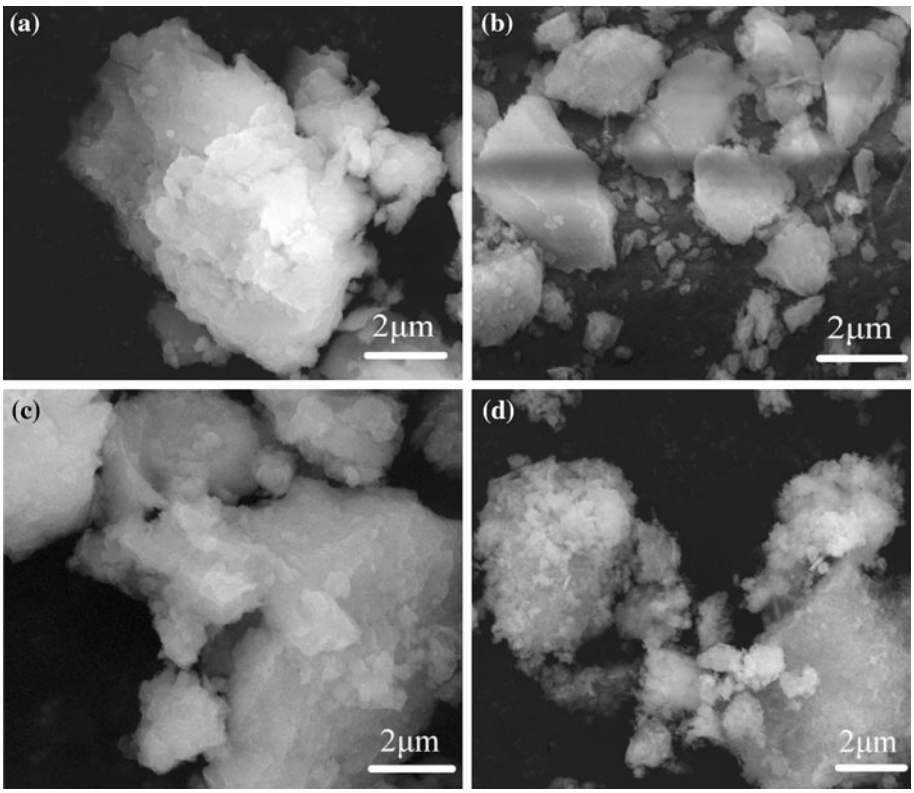

Fig. 6 SEM images of **a** Zn_2–Al, **b** Zn_1–AlEu, **c** Zn_2–AlEu, and **d** Zn_4–AlEu, respectively

The high crystallinity with no impurity phase was at the $Zn^{2+}/(Al^{3+}+Eu^{3+})$ ratios of 2–4. Some intense emissions attributed to transitions $^5D_0$–^7F_J ($J = 1$–4) were observed in all the Eu-doped products, suggesting the permission of $^5D_0$–^7F_J transitions for Eu^{3+} ions in the ZnAl–Cl–LDHs system. It is important as a fluorescent probe for the potential application in biology or medical diagnosis.

Acknowledgements The Project Supported by the National Natural Science Foundation of China (50902067), the Natural Science Foundation of Jiangxi Province (2007GZC1727 and 2008GQH0046), and Program for Innovative Research Team in University of Jiangxi Province.

References

1. Chen H, Zhang F, Fu S, Duan X (2006) Adv Mater 18:3089
2. Silion M, Hritcu D, Popa MI (2009) J Optoelectro Adv Mater 11:528
3. Delorme F, Seron A, Gautier A, Crouzet C (2007) J Mater Sci 42:5799. doi:10.1007/s10853-006-0752-x
4. Crepaldi EL, Pavan PC (2000) J Mater Chem 10:1337
5. Shan D, Wang Y, Zhu MJ, Xue HG, Cosnier S, Wang CY (2009) Biosens Bioelectro 24:1171
6. Tian Y, Wang G, Li F, Evans DG (2007) Mater Lett 61:1662
7. Iyi N, Sasaki T (2008) Appl Clay Sci 42:246
8. Marangoni R, Bouhent MC, Taviot G, Wypych F, Lerouxc F (2009) J Colloids Interface Sci 333:120
9. Nyambo C, Chen D, Su SP, Wilkie CA (2009) Polym Degrad Stab 94:496
10. Vial S, Prevot V, Leroux F, Forano C (2008) Microporous Mesoporous Mater 107:190
11. Dong DW, Jiang SC, Men YF, Ji XL, Jiang BZ (2000) Adv Mater 12:646
12. Chang Z, Evans DG, Duan X, Boutinaud P, De Roy M, Forano C (2006) J Phys Chem Sol 67:1054
13. Gago S, Pillinger M, Sa′ Ferreira RA, Carlos LD, Santos TM, Goncalves IS (2005) Chem Mater 17:5803
14. Sousa FL, Pillinger M, Sa′ Ferreira RA, Granadeiro CM, Cavaleiro AMV, Rocha J, Carlos LD, Trindade T, Nogueira HIS (2006) Eur J Inorg Chem 6:726
15. Zhuravleva NG, Eliseev AA, Lukashin AV, Kynast U, Tretyakov YD (2004) Dokl Chem 396:87
16. Li C, Wang L, Evans DG, Duan X (2009) Ind Eng Chem Res 48:2162
17. Sarakha L, Forano C, Boutinaud P (2009) Opt Mater 31:562
18. Lee KH, Byeon S-H (2009) Eur J Inorg Chem 7:929
19. Gandara F, Puebla EG, Iglesias M, Proserpio DM, Snejko N, Monge MA (2009) Chem Mater 21:655
20. Geng FX, Xin H, Matsushita Y, Ma RZ, Tanaka M, Izumi F, Iyi N, Sasaki T (2008) Chem Eur J 14:9255
21. Geng FX, Matsushita Y, Ma RZ, Xin H, Tanaka M, Izumi F, Iyi N, Sasaki T (2008) J Am Chem Soc 130:16344
22. Benito P, Guinea I, Labajos FM, Rocha J, Rives V (2008) Microporous Mesoporous Mater 110:292
23. Badreddine M, Khaldi M, Legrouri A, Ban'oug A, Chaouch M, De Roy A, Besse JP (1998) Mater Chem Phys 52:235
24. Legrouria A, Lakraimi M, Barroug A, De Roy A, Besse JP (2005) Water Res 39:3441
25. Kooli E, DepiGe C, Ennaqadi A, De Roy A, Besse JP (1997) Clays Clay Miner 45:92
26. Patzko′ A, Kun R, Hornok V, De′ka′′ny I, Thomas E, Norbert S (2005) Colloids Surf A 265:64

27. Lv L, Sun PD, Gu ZY, Du HG, Pang XJ, Tao XH, Xu RF, Xu LL (2009) J Hazard Mater 161:1444
28. Seftel EM, Popovici E, Mertens M, De Witte K, Van Tendeloo G, Cool P, Vansant EF (2008) Microporous Mesoporous Mater 113:296
29. Tao Q, Zhang YM, Zhang X, Yuan P, He HP (2006) J Solid State Chem 179:708
30. Britto S, Radha AV, Ravishankar N, Kamath PV (2007) Solid State Sci 9:279
31. Wang J, Liu Q, Zhang GC, Li ZS, Yang PP, Jing XY, Zhang ML, Liu TF, Jiang ZH (2009) Solid State Sci 11:1597
32. Badreddine M, Khaldi M, Legrouri A, Barroug A, Chaouch M, De Roy A, Besse JP (1998) Mater Chem Phys 52:235
33. Perkkalainena P, Pitkanena I, Huuskonenb J (1999) J Mol Struct 510:179
34. Ramis G, Yi L, Busca G (1996) Catal Today 28:373
35. Delgado RR, Pauli CPD, Carrasco CB, Avena MJ (2008) Appl Clay Sci 40:27
36. Blasse G, Grabmaier BC (1994) Luminescent materials. Springer-Verlag, New York
37. Wang Z, Ströbele M, Zhang KL, Meyer HJ, You XZ, You Z (2002) Inorg Chem Commun 5:230
38. Wang ML, Huang CG, Huang ZH, Guo W, Huang JQ, He H, Wang H, Cao YG, Liu QL, Liang JK (2009) Opt Mater 31:1502
39. Shi QS, Zhang S, Wang Q, Ma HW, Yang GQ, Sun WH (2007) J Mol Struct 837:185